Available online at www.sciencedirect.com
ScienceDirect
Journal of Molecular Catalysis A: Chemical 263 (2007) 1–8
JOURNAL OF MOLECULAR CATALYSIS A: CHEMICAL
www.elsevier.com/locate/molcata

Characterization of stepwise prepared, silica supported zirconocene catalysts designed for olefin polymerization

Jani P.J. Turunen, Tuula T. Pakkanen *

Department of Chemistry, University of Joensuu, P.O. Box 111, FI-80101 Joensuu, Finland

Received 24 February 2006; received in revised form 26 July 2006; accepted 30 July 2006
Available online 12 September 2006

Abstract

Heterogeneous zirconocene catalysts were prepared with an unconventional method by grafting mesoporous silica SBA-15 fiber with $ZrCl_4$ in gas or liquid phase and subsequently with lithium salt of cyclopentadiene (Cp) or indene (Ind). In order to obtain a better understanding of the bonding modes of the zirconium and the ligands, the $ZrCl_x/SiO_2$ and $ZrCl_xL/SiO_2$ were now for the first time characterized by several techniques, including elemental analysis, FTIR spectroscopy, ^{1}H MAS NMR and ^{13}C CP MAS NMR. The results verify the η^5-bonding of the ligands to the metal center, which in turn was discovered to be both mono- and bifunctionally bonded to the silica. The catalysts were tested in ethylene polymerization, in which they yielded polyethylene with moderate activities.

Keywords: Mesoporous silica SBA-15; Metallocene; NMR; Polymerization; Zirconium

1. Introduction

In olefin polymerization, among the best catalysts for the tailoring of the properties of polyolefins are metallocenes. Although metallocene complexes can be used in a homogeneous form, they are often used in the heterogeneous one, i.e. they are supported on an insoluble carrier prior to the polymerization. Typical support materials are silica and alumina, but also magnesium chloride, zeolites, clays, micelles, libid bilayers, liquid or organic crystals and polymers have been used as catalyst carriers [1,2]. The reasons for the heterogenization of the metallocene are, for example, slower deactivation of the metallocene, avoidance of reactor fouling, less cocatalyst required, good and uniform polymer morphology, high polymer density and requirements of the commercial polymerization processes [3].

Methods for heterogenization of the metallocene complex to the support are often divided in three groups: (1) direct immobilization of the metallocene on the support, (2) immobilization on support pretreated with methylaluminoxane (MAO) [4,5] or alkylaluminium [6,7] and (3) activation of metallocene with aluminoxane prior to the immobilization [1,8]. In addition to these three methods, there is also a fourth way to obtain supported metallocene catalyst, namely direct step-by-step preparation of the metallocene on the support surface. This can be done by linking cyclic ligands through a functional group in the ligand or ansa-ligand to the surface and subsequently attaching a metal center to the ligands [9–11]. Or vice versa, as have been done, for example, by Spitz et al. [12,13]. They grafted $ZrCl_4$ onto the silica surface, and then inserted cyclopentadienyl or indenyl ligands to the zirconium, thus producing a heterogeneous zirconocene catalyst. The advantages of this stepwise catalyst preparation method are its simplicity and the possibility to combine a variety of metals and ligands.

In this study we have used a method similar to that of Spitz et al. [12,13] to prepare stepwise cyclopentadienyl and indenyl zirconocene catalysts on a silica surface. However, mesoporous silica fiber was used as the support material due to its high surface area and claimed capability for extrusion polymerization [14]. Differing from the previous studies, the stepwise prepared zirconocene catalysts were characterized by several techniques, including ^{1}H and ^{13}C CP MAS NMR, before the catalysts are being tested in the polymerization of ethylene.

* Corresponding author. Tel.: +358 132 513 340; fax: +358 132 513 390.
E-mail addresses: Jani.P.Turunen@joensuu.fi (J.P.J. Turunen), Tuula.Pakkanen@joensuu.fi (T.T. Pakkanen).

1381-1169/$ – see front matter © 2006 Elsevier B.V. All rights reserved.
doi:10.1016/j.molcata.2006.07.072

2. Experimental

2.1. Materials

Mesoporous silica support, fiber-like SBA-15, was prepared according to the procedure of Zhao et al. [15]. For the removal of the organic template the as-synthesized SBA-15 was calcined at 560 °C in air for 9 h. Nitrogen flow was used during the heating step. Zirconium(IV) chloride (99.95+%) and lithium cyclopentadienide (LiCp, 97%) were purchased from ABCR Chemicals and used as received. Poly(ethylene glycol) (EO)-poly(propylene glycol) (PO) triblock copolymer ($EO_{20}PO_{70}EO_{20}$, M_n ca. 5800), 1.6 M butyllithium in hexane and cyclopentadienyl and indenylzirconium(IV) trichlorides ($CpZrCl_3$ and $IndZrCl_3$, both 97%) were purchased from Aldrich. Toluene, pentane, heptane, tetrahydrofuran (THF) and diethylether (all from Riedel-de Haën) and cyclopentane (Fluka) were dried according to the usual procedures. Methylaluminoxane (10% in toluene, Albemarle) was used without further purification.

Lithium indenide (LiInd) was prepared [16] by adding equal amount of butyllithium (1.6 M in hexane, Aldrich) to indene (99+%, Aldrich) under argon atmosphere. Both reagents were first diluted in diethylether and cooled to −70 °C. The mixture was mixed for 22 h and allowed slowly to warm up to room temperature. Solvent was evaporated in vacuum, dry cyclopentane added and the solution cooled to −70 °C, which led to the precipitation of the lithium indenide. Slightly pink product was recovered by decantation and drying in a vacuum. ^{13}C CP MAS NMR signals of the solid lithium indenide were observed at 122.2, 112.3 and 93.1 ppm.

2.2. Catalyst preparation

Silica support (1.5 g) was mixed with $ZrCl_4$ (0.38 g for silica A and 0.75 g for silica B) and placed in a quartz tube. Vacuum was introduced to the tube, the valves were closed and the tube was placed in an oven at 300 °C. After 30 min, a dynamic vacuum was introduced for 30 min to remove the unreacted $ZrCl_4$. The tube was filled with nitrogen and transferred into a nitrogen glove box. The product was washed with 4× 20 ml of boiling toluene or THF to further remove unreacted $ZrCl_4$, then dried in vacuum at 150 °C.

The lithium salt of the desired ligand (LiCp or LiInd) was dissolved in a small amount of THF (2–3 ml) and pipetted on 1.2 g of the zirconium-modified silica support (V_{pore} = 0.5–1.0 cm^3/g). After 2 h of diffusion of the solution into the pores, 20 ml of toluene was added and the suspension shaked at 50–80 °C under argon overnight. The product was then filtered and washed with 4× 20 ml of toluene, dried in vacuum and washed with 2× 15 ml of pentane to remove the toluene residues. Then it was dried again at 50 °C in vacuum. The final products are here called catalysts, even though without activation they are actually catalyst precursors.

2.3. Ethylene polymerization

The polymerizations were made with a 500 ml Büchi stainless steel reactor with the following way: the catalyst in 10 ml of heptane and the cocatalyst MAO (Al/Zr = 1000) were packed in separate stainless steel catalyst containers in a nitrogen glove box. Heptane (250 ml) was transferred under an inert atmosphere into the evacuated reactor and heated to the desired polymerization temperature (80 °C). Both the catalyst and cocatalyst were transferred into the reactor using a nitrogen overpressure. Under 400 rpm stirring, the catalyst was allowed to activate for 5 min before 5 bars of ethylene was introduced to the reactor, simultaneously raising the stirring rate to 600 rpm. During the polymerization the temperature was kept constant as well as the partial pressure after it had reached the set value. The calculations of polymerization activity were based on the average ethylene pressure (3.63–4.76 bar), measured by the computer coupled with the reactor. The reaction was terminated by venting ethylene, opening the reactor and then by adding ethanol. The polymer was stirred in acidic (HCl) ethanol solution for 3–4 h, filtered, washed with ethanol and dried at room temperature.

2.4. Characterizations

BET surface area, pore size, pore size distribution and pore volume of the silica were determined by nitrogen physisorption using a Micromeritics ASAP 2010. The samples were degassed at 155 °C for at least 3 h, preferably overnight. A Nicolet Impact 400D FTIR spectrometer, connected to a nitrogen glove box and equipped with a DRIFT unit, was used to evaluate the presence of hydroxyl groups on the silicas and catalysts. Measurements were performed under a nitrogen atmosphere, the sample being undiluted and measured on a mirror plate. A Chemagnetics CMX 400 MHz Infinity, Chemagnetics CMX 270 MHz Infinity and Bruker Avance 400 MHz spectrometers were used in the characterization of the silica and the catalyst and in the quantitative determination of the hydroxyl groups and cyclic ligands. Zirconia rotor systems with diameters of 6 or 7 mm were used in the measurements.

Zirconium contents of the catalysts were determined with a TJA IRIS ICP-AES (Offenbach, Germany) and chloride by a potentiometric titration with $AgNO_3$. SEM images of the silica support were obtained with a Hitachi S4800 scanning electron microscope. The zirconium distribution in the silica was determined with a SEM-EDS (JEOL 840 with a PGS EDS analysator at Fortum Oil & Gas Oy, samples casted in Epofix resin, microtomed and sputtered with carbon). Molecular weights were determined by the measurement of dilute solution viscosity (decalin, 135 °C) with a capillary viscometer as described in ASTM D 1601 [17]. Antioxidant BHT (0.2 wt.%) was added in the decalin in order to avoid oxidation of the polymer. The solution concentration was 15–98 mg dl^{-1} and the polymer samples were dissolved at 165–185 °C under nitrogen atmosphere. The nominal molecular weights were calculated using Mark-Houwink constants $K = 62 \times 10^{-3}$ ml g^{-1} and $\alpha = 0.700$ [18]. Melting points were determined with a Mettler-Toledo DSC821e (Zürich, Switzerland) differential scanning calorimeter using a scanning rate of 10 K/min.

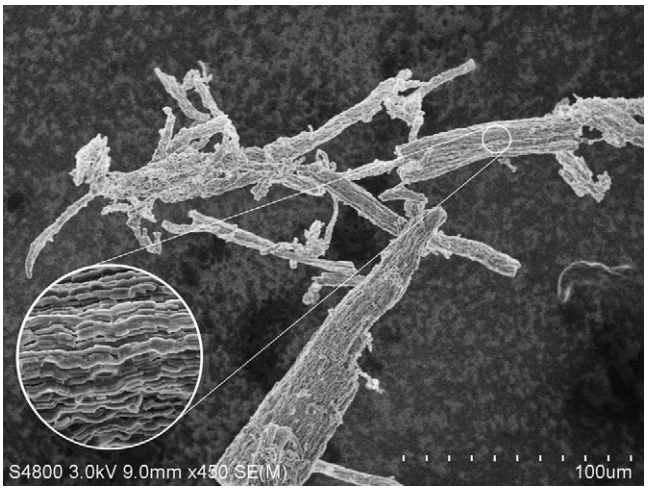

Fig. 1. SEM image of mesoporous SBA-15 silica fibers.

3. Results and discussion

3.1. Preparation and characterization of zirconium-modified silica

Inspection of the SBA-15 type silica support with a SEM revealed a rope-like structure (Fig. 1). The average length of the ropes was 10–150 μm and thickness 2–20 μm. The ropes consisted of intertwined, parallel aligned bundle of wires (thickness 300–400 nm), in which the tubular mesopores are hexagonally ordered and oriented parallel to the fiber axis. BET surface area of 930 m^2/g, average pore diameter of 57 Å and pore volume of 1.18 cm^3/g were determined by nitrogen physisorption. According to ^1H MAS NMR measurements, the hydroxyl group surface densities were 1.5 and 0.34 OH/nm^2 for isolated and hydrogen bonded SiOH, respectively (silica A). Two synthesis batches of silica (Table 2) were used for different catalyst compositions, but due to identical synthesis conditions there were no remarkable differences in the surface properties.

Zirconium(IV) chloride was grafted on the silica surface in gas phase at 300 °C, the reaction going as follows:

$$n\text{Si–OH} + \text{ZrCl}_4 \rightarrow (\text{Si–O})_n\text{ZrCl}_{4-n} + n\text{HCl}; \quad n = 1, 2 \tag{1}$$

The formation of ZrO_2 during the grafting cannot be disclosed, as the 300 °C has been found to be an adequate temperature for the formation of some ZrO_2 from $ZrCl_4$ on silica [19]. Washing of the as-synthesized, white product with toluene turned it yellow and washing with THF light brown. Some physisorbed $ZrCl_4$ may have remained on the silica at this stage, but later when the insertion of cyclic ligands turns the zirconium complex into a more soluble form, the physisorbed $ZrCl_4$ is removed. The final precatalyst was considered to be free of non-bonded zirconocene.

SEM-EDS was useful in confirming the dispersion of zirconium chloride in the silica fiber (Fig. 2). An elemental analysis from the cross-section of a silica fiber showed an even distribution of Zr, which proved the $ZrCl_4$ had reached also the inner pore surface of the support, not just the outer fiber surface. Since the microtomed samples were exposed to air, chlorine may have escaped as HCl and did not show up clearly in all the images.

The results from zirconium and chloride content analysis are presented in Table 1. The Cl/Zr molar ratios 2.5 and 2.6 of the

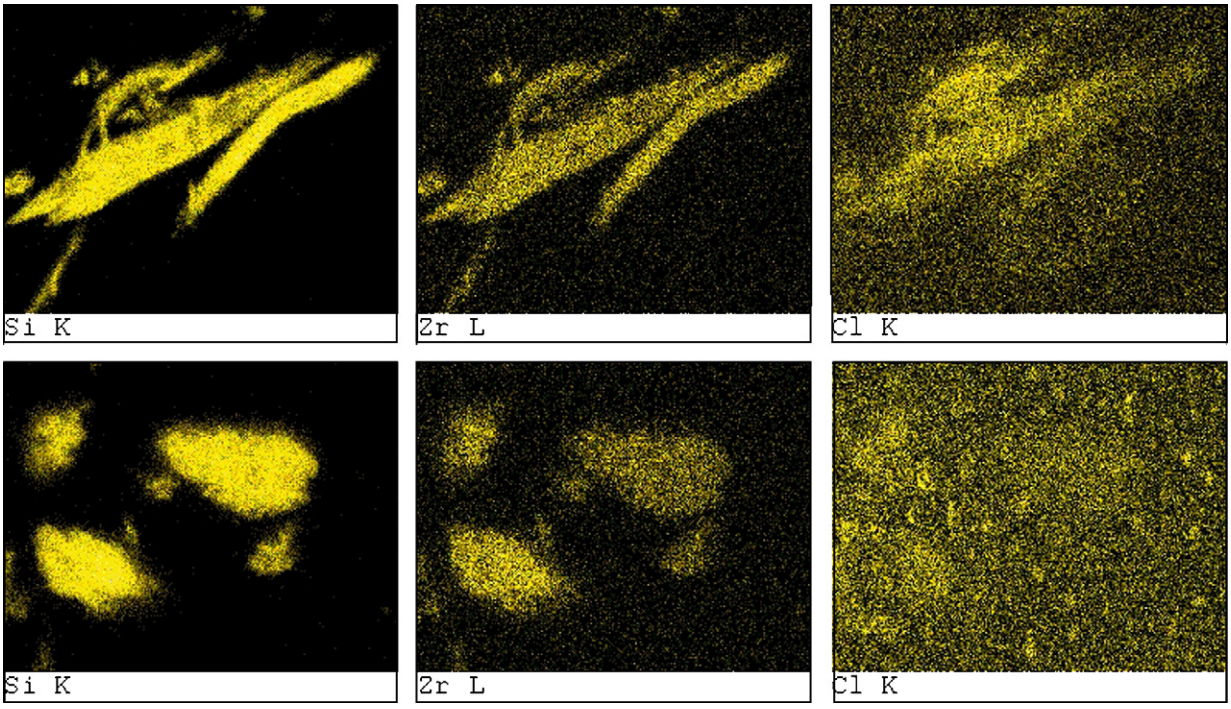

Fig. 2. SEM-EDS images of zirconium-modified silica fibers showing distributions of silicon, zirconium and chlorine (Si, Zr and Cl). In the upper row the fibers have been microtomed along the fiber axis, in the lower row perpendicular to the fiber axis.

Table 1
Measured zirconium and chloride contents of zirconium-modified silicas

Support	Zr (wt.%)	Cl (wt.%)	Cl/Zr molar ratio
A	6.8	6.5	2.5
B	11.2	11.3	2.6

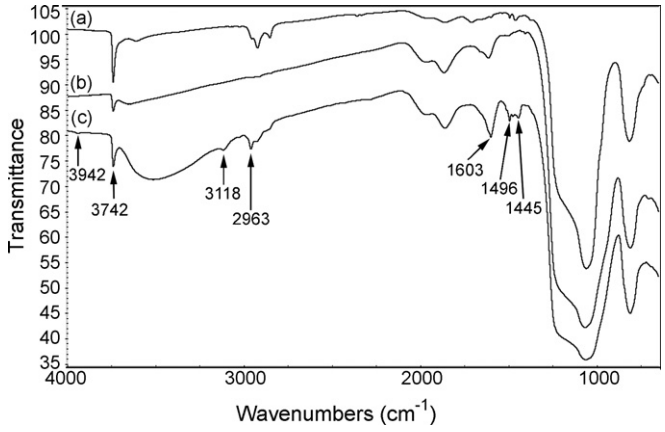

Fig. 3. FTIR spectra of (a) pure mesoporous silica, (b) zirconium-modified silica and (c) Zr–silica after Cp ligand insertion (catalyst AZ-Cp3).

supports indicate the zirconium is both mono- and bifunctionally bonded to the surface. However, in interpretation of the bonding mode of zirconium based merely on Cl/Zr ratio, also the possible formation of ZrO_2 and Si–Cl bonds [20] has to be considered.

Nitrogen physisorption was used to determine the changes in the BET surface area, average pore diameter and pore volume of the silica caused by the grafting with $ZrCl_4$ (Table 2). The results clearly show that surface area and pore volume decreased, and average pore diameter increased, as expected. Normally one would expect a decrease in the pore diameter due to the incorporation of $ZrCl_4$, but in the case of SBA-15 it is not so. The tubular mesopores of the SBA-15, namely, are interconnected with micropores [21], which are clogged in the grafting with the $ZrCl_4$. As the pore diameter presented in Table 2 is calculated as an average value, disappearance of the micropores (observed in the pore size distribution graph) leads to a higher d_{pore} value. The change is especially clear for support BZ, which has almost twice the zirconium concentration of AZ.

Fig. 3b shows an FTIR spectrum of mesoporous silica after incorporation of zirconium into the pore surfaces. Comparison to the spectrum of pure silica, Fig. 3a, reveals consumption of OH-groups (sharp signal at 3742 cm^{-1} for isolated OH and broad signal at ~3600 cm^{-1} for hydrogen bonded OH) during $ZrCl_4$ treatment, as expected. The formation of Si–O–Zr linkages should be observed at 950 cm^{-1} [22], but it is unfortunately

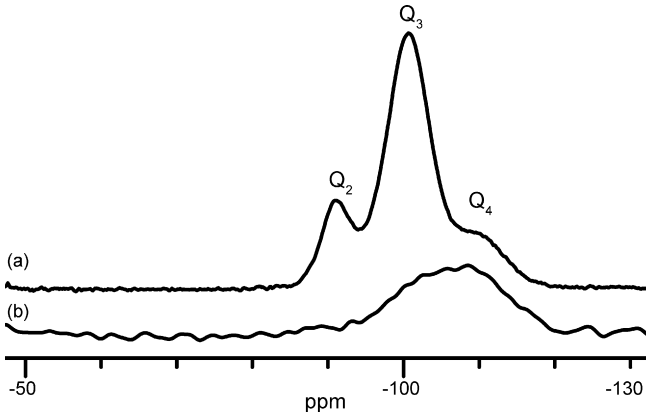

Fig. 4. ^{29}Si CP MAS NMR spectra of (a) pure SBA-15 silica fiber and (b) zirconium-modified SBA-15 silica fiber.

in the same area where also the Si–O–Si band exists. The vibrations at 2960–2850 cm^{-1} in spectrum 3a are probably due to C–H stretching of residual organic fragments of the triblock copolymer template, which have been trapped inside the silica structure and thus have not been fully removed despite calcination [23].

As can be observed in spectrum 3b and Table 4, the consumption of the isolated hydroxyl groups is not complete even though enough $ZrCl_4$ is used to obtain a zirconium loading of 12–13 wt.% in the silica. The OH concentration of silica A before the $ZrCl_4$ reaction was 0.34 H-bonded and 1.5 isolated OH/nm^2, which, in theory, would allow 0.66 g of $ZrCl_4$ to react with 1 g of the silica. The calculation is based on the assumption that there are no inaccessible OH groups and that $ZrCl_4$ reacts monofunctionally with all of the hydroxyl groups. In that case, the theoretical saturation limit of zirconium is 16.6 wt.% for this particular silica. The presence of inaccessible OH groups, however, cannot be disclosed.

The zirconium-modified silica was characterized also by ^{29}Si NMR spectroscopy (Fig. 4). Measurements with both the CP MAS and ordinary decoupled pulse program confirmed the reaction of surface hydroxyls as reduction of the Q_3 silicon atoms, indicating the formation of Zr–O–Si linkages. No change was observed in the inner Q_4 atoms, which suggests that the zirconium has not drifted deeper into the silica structure, i.e. it is present only on the pore surface.

3.2. Insertion of ligands

Next step in catalyst preparation was to insert the cyclic ligands, cyclopentadienyl and indenyl, to the zirconium-modified silica surface. The amounts of ligand (LiCp and LiInd) salts were set to correspond to 500–600 and 800–1300 μmol/g of silica for

Table 2
Effect of zirconium modification on the surface area, pore volume and pore diameter of mesoporous silica

Sample[a]	Zr (wt.%)	S_{BET} before (m^2/g)	S_{BET} after (m^2/g)	d_{pore} before (Å)	d_{pore} after (Å)	V_{pore} before (cm^3/g)	V_{pore} after (cm^3/g)
AZ	6.8	929	685	57.4	56.1	1.18	0.99
BZ	11.2	891	344	42	57	0.94	0.49

[a] Letter Z in the name of the sample denotes modification with $ZrCl_4$.

Table 3
Measured zirconium, chloride and ligand contents of the catalysts

Catalyst	Cyclic ligand concentration (μmol/g_{silica})[a]	Zr (wt.%)	Cl (wt.%)	Cl/Zr	Cl/Zr before ligand immobilization
AZ-Cp1	240	6.7	6.2	2.4	2.5
BZ-Ind	67	10.0	9.7	2.5	2.6

[a] Ligand concentration determined with ^{1}H MAS NMR.

Cp and Ind, respectively. After washing and drying, the zirconium, chloride and ligand contents of the catalyst were analyzed again (Table 3). The Cl/Zr ratio of the support does not change much, mainly due to the high excess of Zr and Cl on the support compared to the cyclic ligands.

Four different Cp catalysts were prepared. Three of them were prepared as previously described but one was prepared grafting $ZrCl_4$ in toluene suspension instead of gas phase (AZ-Cp2). The best method to evaluate the amount of cyclic ligands bonded to the silica surface turned out to be ^{1}H solid state NMR spectroscopy. Conventional carbon analysis could not be used due to presence of some coordinated THF, which could not be removed without a possible decomposition of the catalyst.

The zirconium and Cp ligand concentrations are listed in Table 4. An interesting finding is that in the five Cp-catalysts prepared, the Zr/Cp molar ratio is the same (3.0), irrespective of the zirconium concentration on the support and of the amount of Cp used in the reaction. In AZ-Cp2 the amount of Cp used in the catalyst preparation was 600 μmol/g, in the other catalysts it was 500 μmol/g. Apparently a Cp ligand occupies a space of three zirconium chloride groups on the surface. In this case most of the zirconium species seems to be closely packed, in other words existing as islands. If the zirconium species were scattered on the surface with long intermolecular distances, the Zr/Cp ratio would probably be smaller. The saturation density of cyclopentadienyl on the zirconium-modified silica surface (Cp/nm^2) thus depends on the zirconium concentration, which in turn, naturally depends on the density of hydroxyl groups on the surface.

Fig. 3c shows an FTIR spectrum of catalyst AZ-Cp3. Compared to the zirconium-modified silica, a broad signal at 3700–3200 cm^{-1} has appeared. It is possible this signal originates from the remaining hydroxyl groups of the silica perturbed by hydrogen bonding interactions with oxygen atoms of coordinated THF [24]. In addition, the partially positive hydrogen atoms of the hydroxyl groups may also interact with the negative chlorides of lithium chloride, which is formed in the reaction of surface Zr–Cl and lithium salt of the ligand. LiCl is non-soluble in toluene and THF and thus remains in the pores of the silica.

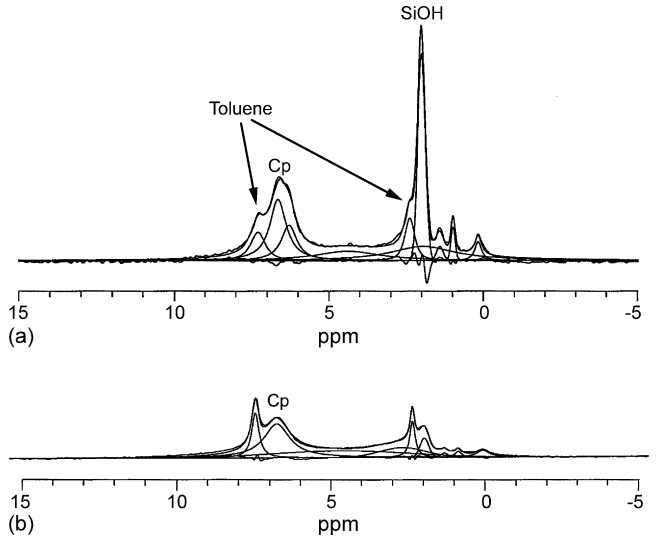

Fig. 5. ^{1}H MAS NMR spectra of two cyclopentadienyl zirconium catalysts (a) AZ-Cp1 and (b) AZ-Cp4 with signal deconvolutions.

Since the concentration of Cp ligand on the support is very low, the Cp vibrations in IR will also be very weak. In addition, most of the signals of Zr–Cp lie at the same wave numbers as those of silica, so they are mostly obscured. An IR vibration of η^5-bonded Cp ligand is typically observed at 3946 cm^{-1} [24], where indeed a very weak signal exists (Fig. 3c). Other signals of Cp ring due to the C–H stretching and symmetric distortion of C–C bonds are typically observed at 3100 and 1443 cm^{-1}, respectively [22,25]. In spectrum 3c, these two signals are observed as weak vibrations at 3118 and 1445 cm^{-1}.

Solid state ^{1}H and ^{13}C NMR spectroscopy was used to evaluate the structure and bonding of the Cp and Ind ligands on the zirconium-modified silica surface. Examples of the NMR spectra are shown in Figs. 5 and 6. The signals of the coordinated

Table 4
Cyclopentadienyl and SiOH concentrations of the catalysts according to ^{1}H MAS NMR

Catalyst	Number of SiOH on the catalyst (×10^{20} OH/g)	Number of Cp rings on the catalyst (×10^{20} Cp/g)	Amount of Cp on the catalyst (μmol/g)	Zr concentration (μmol/g)	Zr/Cp molar ratio
AZ-Cp	4.9	1.5	240	730	3.0
AZ-Cp2[a]	–	2.6	430	1280	3.0
AZ-Cp3	1.0	2.7	440	1300	3.0
AZ-Cp4	6.3	2.7	440	1320	3.0
Silica A[b]	17.1	–	–	–	–

[a] Zirconium grafted in a toluene.
[b] SBA-15 silica, support A.

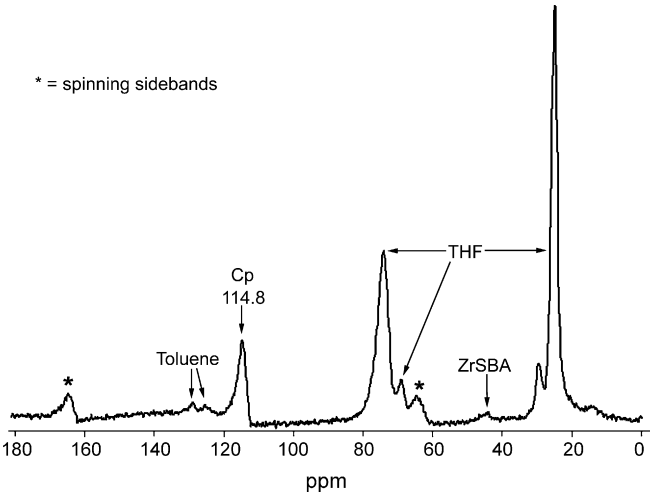

Fig. 6. ^{13}C CP MAS NMR spectra of a cyclopentadienyl zirconium catalyst (sample AZ-Cp2).

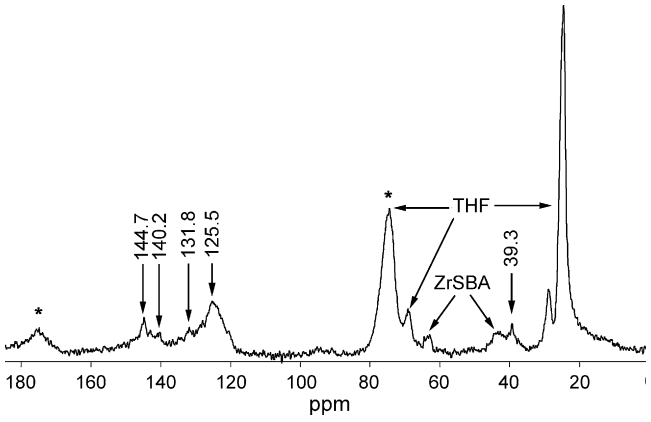

Fig. 7. ^{13}C CP MAS NMR spectrum of indenyl catalyst BZ-Ind. The asterisk denotes spinning sidebands.

THF are visible especially in the ^{13}C NMR spectra at 75 and 25 ppm. Resonances of free THF are observed at 68 and 26 ppm (not much present in our catalysts).

In ^{1}H MAS NMR the resonances of Cp-rings are rather broad, which implies they are rather restricted in motion. In addition, the ^{13}C CP MAS NMR spectra show spinning sidebands from the Cp ring, which rules out isotropic motion of the ring (Fig. 6). The chemical shift at 114.8 ppm is characteristic for zirconium bonded Cp ligand [22] and differs from that of LiCp (106.0 ppm). According to these results, one could draw a conclusion the rings are bound to the surface and there on zirconium.

In some samples, e.g. AZ-Cp1 (Fig. 5a), the ^{1}H NMR signal due to hydrogen atoms in the Cp ring seemed to consist of at least two signals. The most probable explanation for the two Cp signals is the presence of the Cp ligands in two different chemical environments, i.e. either in mono- or bifunctionally bonded zirconium. On the other hand, one could also suggest that a possible explanation for the two signals is a η^1-bonding due to the reaction of a single carbon in the Cp ring instead of a η^5-bonding of the whole ring system. Only one η^1-bonded Cp ligand, however, makes the zirconium atom electron-deficient. Unless more than one Cp ligand has been bonded to the same metal center and one of them is η^5-bonded, monohapto bonding is improbable. In addition, it has been shown that the η^1-bonded Cp ligand can be down to −87 °C fluxional enough to show only one ^{1}H and ^{13}C NMR signal [26,27], which is at the same ppm value as the signal of η^5-bonded Cp ligand. Thus, in measurements made at room temperature, it is very unlikely to see more than one peak in the ^{1}H NMR spectra even if the Cp ligands were η^1-bonded.

The ^{13}C MAS NMR spectra of the indenyl catalyst showed weak signals for the cyclic ligands when compared to those of the Cp catalysts. Lithium indenide is only poorly soluble in THF (or any other organic solvent we tested), so possibly the ligand salts have not properly reached the Zr–Cl groups in the pores of the support. The strongest ^{13}C MAS NMR signal in the spectrum of the indenyl catalysts was observed at 125 ppm, but weak resonances were detected also at 144–140, 132 and 39 ppm (Fig. 7). These weak signals are at different ppm values than those typically reported for indenyl ligands η^5-bonded to zirconium (135–100 ppm) [28–30]. Since indene has signals at 145, 144, 134, 132, 126–121 and 39 ppm in the ^{13}C spectrum, it is reasonable to suggest that part of the lithium indenide is somehow converted to indene. The weak signals in the spectrum are also narrow, which suggests that they originate from a mobile molecule. One could suggest that the lithium indenide may have reacted with the residual silanols of the surface, that has yielded indene. In that case the same reaction could take place also with LiCp, yielding dicyclopentadiene. Dicyclopentadiene, however, could not be observed in the ^{13}C CP MAS NMR spectra, perhaps due to its possible volatility (b.p. 170 °C). Nevertheless, the strong signal at 125.5 ppm in Fig. 7 verifies that most of the indenyl ligands have been bonded to the zirconium.

3.3. Ethylene polymerization

In order to find out the catalytic activity of the prepared catalysts they were activated with MAO (Al/ligand = 1000) and used in the polymerization of ethylene. Table 5 summarizes the polymerization results. Polymerization activity is the most useful result when one wishes to evaluate the number on active centers on the catalyst surface, but polydispersity M_w/M_n, on the other hand, gives idea of the number of different kinds of active centers on the catalyst. Unfortunately, due to low polymerization yields, the amounts of catalyst residues in some of the polymerization products were high, which led to the clogging of the filters of the gel permeation chromatograph (GPC). In addition, the samples with the highest molar masses did not dissolve properly in trichlorobenzene which also prevented the use of GPC. Thus the average molar masses of the samples were determined with a capillary viscometer, and therefore no M_w/M_n results are available.

The zirconium-modified silica without any cyclic ligands (ZrSBA) polymerizes ethylene with low activity in the presence of MAO (Table 5), as reported also by Spitz et al. [12]. The molar mass of the polyethylene prepared with ZrSBA as the catalyst is 3.76 million, already in the range of UHMWPE. Since Kageyama et al. [14] discovered the capability of Cp_2Ti-MSF (mesoporous silica fiber) to produce UHMWPE (M_v = 6.2

Table 5
Polymerization results

Catalyst	Amount of catalyst (μmol)	Time (min)	Yield (g)	Activity (kg/(mol h bar))	Productivity (g_{PE}/g_{cat}, h)	T_m (°C)	Crystallinity (%)	Molar mass (kg/mol)
Homog. Cp_2ZrCl_2	3.0[a]	10	6.30	3470	43000	143.0	74	170
ZrSBA	22[b]	30	0.38	7	41	139.4	46	3760
AZ-Cp	8.0[b]	30	3.04	160	190	140.2	69	228
AZ-Cp2	8.0[b]	30	8.60	460	930	139.1	66	137
BZ-Ind	4.0[b]	40	2.31	181	57	141.9	54	1180
$CpZrCl_3/SiO_2$	8.0[a]	30	2.67	140	170	140.9	59	313
$IndZrCl_3/SiO_2$	8.0[a]	30	0.73	38	56	141.4	63	1520

In all polymerizations Al/ligand = 1000, $T = 80\,^{\circ}C$, $p_{average} = 3.6$–4.8 bar.
[a] Amount of catalyst corresponds to zirconium.
[b] Amount of catalyst corresponds to that of Cp or Ind, determined with ^1H MAS NMR.

million), it is unclear whether this 3.76 million is a partial result of the mesoporous support or a sole product of the zirconium chloride on the silica surface. As can be observed from Table 5, the incorporation of cyclic ligands to the ZrSBA increases the polymerization activity of zirconium chloride. This effect can be considered as further evidence, that the ligands are bonded to zirconium.

The polymerization activities of the prepared actual catalysts are far from those obtained from homogeneous polymerizations with Cp_2ZrCl_2. This is a common phenomenon with supported metallocenes and results, for example, from steric hindrance and increased bond energies in the transition state of the active site [31]. Of our catalysts the most active is AZ-Cp2, which was prepared by immobilizing the zirconium chloride on an SBA-15 type silica with the adsorption in toluene, and the Cp rings were attached with the incipient wetness method using THF as the solvent. The polymerization activities of stepwise prepared catalyst are about the same (Cp) or higher (Ind) than those obtained by commercial zirconocene trichloride complexes adsorbed on silica.

Leaching is also a common problem with supported metallocenes whenever alkylaluminums or methylaluminumoxane (which always contain free trimethylaluminum) are used. The reaction of alkylaluminums result in the cleavage of the Si–O bond, which leads to the desorption of the active metallocene from the support [32]. This, in turn, leads to a partial polymerization in homogeneous media and thus to a more heterogeneous product, not to mention the reactor fouling. Unfortunately in many research articles describing a MAO-cocatalyzed polymerization with heterogenized metallocene catalyst, the leaching study has been omitted and therefore it is not known whether the metallocene actually remains on the support during the polymerization. In this study, to observe whether part of the active catalyst component is desorbed during the polymerization, the catalyst, MAO and heptane were stirred in a 500 ml glass reactor at 80 °C under nitrogen for the same time as the polymerization would take place. The mixture was then filtered in a nitrogen glove box and transferred into a 250 ml Büchi stainless steel polymerization reactor for ethylene polymerization. No additional MAO was used in the polymerization. This leaching experiment with the cyclopentadienyl catalyst revealed that part of the catalyst desorbed from the support during the polymerization. The polymerization activity of the leaching experiment (88 $kg_{PE}/(mol\,h\,bar)$) is, however, only about 10% of the corresponding normal polymerization with the heterogeneous catalyst (920 $kg_{PE}/(mol\,h\,bar)$). The amount is relatively low, keeping in mind that the leached metallocene is in homogeneous media, thus producing ethylene with far higher activity than the parent heterogeneous catalyst. Of course, part of the leached species may have been deactivated during the handling and filtering, so this method of studying the leaching cannot be used as an exact measure of the desorbed metallocene. Another method [33] of studying the leaching would be the determination of metal content on the catalyst prior to and after the reaction with MAO, but the adsorption of the MAO on the silica makes that method unreliable too.

4. Conclusions

In this study we stepwise prepared heterogeneous zirconocene catalysts by bonding the metal center first onto mesoporous silica fiber, followed by insertion of cyclic ligands to the metal. To the best of our knowledge, this was the first time the catalysts prepared with this method were characterized by several techniques. Insertion of cyclopentadienyl ligands on zirconium-modified mesoporous silica succeeded well, indenyl ligands in lesser extent. The use of other synthesis procedures or wider pore silica might enhance bonding of indenyl ligand too. According to IR and NMR measurements both ligand types were bonded to the zirconium, and the results specifically point to the η^5-bonding. Coordinated THF is also present on the zirconium-modified silica surface, but according to NMR spectra there is no evidence THF is still present in those metal centers where a cyclic ligand has bonded.

When activated with MAO, the $ZrCl_4$-modified silica produces ultra-high-molecular-weight polyethylene, yet with very low polymerization activity. Insertion of Cp or Ind ligands significantly increases the activity, which is further evidence the ligands are bonded to the zirconium. Polymerization activities of the prepared catalyst are also slightly improved compared to the commercial zirconocene trichlorides grafted directly onto silica. Molar masses and melting points of the polymers produced with stepwise prepared Cp and Ind catalysts were similar to those of polyethylenes obtained with impregnated $CpZrCl_3$

and $IndZrCl_3$. On the whole, the main advantage of this stepwise catalyst preparation is the ability to prepare various metal–ligand combinations on the silica surface, especially such that could not be obtained by impregnating a commercial metallocene complex on a support. Furthermore, this catalyst preparation method is a good way to examine the effect of different ligand–metal combinations on the polymerization activity and on the structure and properties of the polymer formed.

Acknowledgement

The authors wish to thank Dr. Andrew Root for the measurement and interpretation of some of the NMR spectra.

References

[1] G.G. Hlatky, Chem. Rev. 100 (2000) 1347.
[2] K. Tajima, T. Aida, Chem. Commun. (2000) 2399.
[3] J.C.W. Chien, Top. Catal. 7 (1999) 23.
[4] D. Bianchini, K.M. Bichinho, J.H.Z. dos Santos, Polymer 43 (2002) 2937.
[5] K.S. Lee, C.-G. Oh, S.-K. Yim, J. Ihm, J. Mol. Catal. 159 (2000) 301.
[6] R. van Grieken, G. Calleja, D. Serrano, C. Martos, A. Melgares, I. Suarez, Polym. React. Eng. 11 (1) (2003) 17.
[7] M. de Fatima, V. Marques, M.J. de Alcantara, J. Polym. Sci. A: Polym. Chem. 42 (2004) 9.
[8] G. Fink, B. Steinmetz, J. Zechlin, C. Przybyla, B. Tesche, Chem. Rev. 100 (2000) 1377.
[9] H. Juvaste, T.T. Pakkanen, E.I. Iiskola, Organometallics 19 (23) (2000) 4834.
[10] A.-M. Uusitalo, T.T. Pakkanen, E.I. Iiskola, J. Mol. Catal. A: Chem. 177 (2002) 179.
[11] M.O. Kristen, Top. Catal. 7 (1999) 89.
[12] R. Spitz, N. Verdel, V. Pasquet, J. Dupuy, J.P. Broyer, T. Saudemont, in: W. Kaminsky (Ed.), Metallorganic Catalysts for Synthesis, Polymerization: Recent Results by Ziegler-Natta, Metallocene Investigations, Springer-Verlag, 1999, pp. 347–357.
[13] R. Spitz, V. Pasquet, J. Dupuy, J. Malinge, US Pat. 5739226 (1996).
[14] K. Kageyama, J. Tamazawa, J. Aida, Science 285 (1999) 2113.
[15] D. Zhao, J. Sun, Q. Li, G.D. Stucky, Chem. Mater. 12 (2000) 275.
[16] R.E. Dinnebier, S. Neander, U. Behrens, F. Olbrich, Organometallics 18 (1999) 2915.
[17] Standard Test Method for Dilute Solution Viscosity of Ethylene Polymers, D 1601, Annual Book of ASTM Standards, American Society for Testing and Materials, 1981.
[18] M. Kurata, Y. Tsunashima, in: J. Brandrup, E.H. Immergut, E.A. Grulke (Eds.), Polymer Handbook, 4th ed., J. Wiley & Sons, New York, 1999, p. VII/8.
[19] (a) A. Kytökivi, S.J. Haukka, J. Phys. Chem. B 101 (1997) 10365;
(b) A. Kytökivi, E.-L. Lakomaa, A. Root, Langmuir 12 (1996) 4395;
(c) A. Kytökivi, E.-L. Lakomaa, A. Root, H. Österholm, J.-P. Jacobs, H.H. Brongersma, Langmuir 13 (1997) 2717.
[20] S. Haukka, E.-L. Lakomaa, A. Root, J. Phys. Chem. 97 (19) (1993) 5085.
[21] K. Miyazawa, S. Inakagi, Chem. Commun. (2000) 2121.
[22] M. Kröger-Laukkanen, M. Peussa, M. Leskelä, L. Niinistö, Appl. Surf. Sci. 183 (2001) 290.
[23] J.C. Ro, I.J.J. Chung, Non-Cryst. Solids 130 (1991) 8.
[24] (a) E.I. Iiskola, S. Timonen, T.T. Pakkanen, O. Härkki, J.V. Seppälä, Appl. Surf. Sci. 121/122 (1997) 372;
(b) E.I. Iiskola, S. Timonen, T.T. Pakkanen, O. Härkki, P. Lehmus, J.V. Seppälä, Macromolecules 30 (1997) 2853.
[25] F.G. Costa, E.A. Braga, S.T. Brandão, A. de Freitas Espeleta, Z.N. da Rocha, L.M.T. Simplício, E.A. Sales, Appl. Catal. A 290 (2005) 221.
[26] C.P. Casey, J.M. O'Connor, W.D. Jones, K.J. Haller, Organometallics 2 (1983) 535.
[27] E.J. Munson, M.C. Douskey, S.M. De Paul, M. Ziegeweid, L. Phillips, F. Separovic, M.S. Davies, M.J. Aroney, J. Organomet. Chem. 577 (1999) 19.
[28] M.A. Schmid, H.G. Alt, W.J. Milius, Organomet. Chem. 514 (1996) 45.
[29] Y. Zhang, J. Huang, X. Yang, J. Zhang, Y. Qian, J. Polym. Sci. A: Polym. Chem. 43 (2005) 1261.
[30] S.K. Noh, J. Kim, J. Jung, C.S. Ra, D.-h. Lee, H.B. Lee, S.W. Lee, W.S. Huh, J. Organomet. Chem. 580 (1999) 90.
[31] W. Kaminsky, H. Winkelbach, Top. Catal. 7 (1999) 61.
[32] R. Mulhaupt, J. Calabrese, S.D. Ittel, Organometallics 10 (1991) 3403.
[33] W. Kaminsky, C. Strübel, J. Mol. Catal. A: Chem. 128 (1998) 191.